Synthesis of Rhodium-carbonyl Complexes Bearing a Novel P,N-Chelating Ligand of Schiff-base Type

Takahiro Sasamori,* Teruyuki Matsumoto, and Norihiro Tokitoh

Institute for Chemical Research, Kyoto University, Gokasho, Uji, Kyoto 611-0011, Japan

*Corresponding author. Tel: +81 774 38 3202; Fax: +81 774 38 3209.

E-mail address: sasamori@boc.kuicr.kyoto-u.ac.jp

Abstract

Schiff-base type N,P-chelating ligands, phosphorus analogues of imino-anilido ligands, were designed and synthesized as a new type of ligands toward transition metals, and the rhodium-carbonyl complexes bearing the novel imino-phosphido and phosphaalkenyl-anilido ligands were synthesized as stable crystalline compounds. Their structures were definitively revealed by X-ray crystallographic analysis, showing the unique electronic features of the ligands. In addition, the effective trans-influence of the phosphorus atom was suggested on the basis of the structural parameters and spectroscopic features of the isolated complexes.

Keywords: Schiff base; Phosphorus; Phosphaalkene; Rhodium; Steric protection; Trans-influence

1. Introduction

Schiff-base-type N,N'-chelating ligands such as β-diketiminato and imino-anilido ligands (Scheme 1) have been utilized for the stabilization of unique species of transition metals and main group elements [1]. Thus, the coordination chemistry of the Schiff-base ligands has attracted much interest in the research field of not only fundamental chemistry but also industrial chemistry from the viewpoints of supporting ligands of the catalysts for olefin polymerization [2]. The features of the β-diketiminato and imino-anilido ligands can be

mentioned as follows: (i) facile preparation, (ii) strong coordination ability to the central atom in a monovalent and bidentate fashion, (iii) steric effect afforded by the substituents on the nitrogen atoms, (iv) electronic effect due to the π-electron conjugation in the cyclic skeleton of the resulting complexes.

<insert Scheme 1 here>

On the other hand, the coordination chemistry of low-coordinated organophosphorus compounds has drawn a great deal of recent attention due to their unique electronic features, i. e., the characteristic low-lying π*-orbital level [3]. Generally, low-coordinated organo-phosphorus compounds are highly reactive toward oxygen and moisture and difficult to be handled under ambient conditions due to their extremely high reactivity toward self-oligomerization. However, several numbers of low-coordinated organophosphorus compounds such as phosphaalkenes (P=C) and diphosphenes (P=P) have been synthesized and isolated as stable compounds by taking advantage of kinetic stabilization using bulky substituents [4], since the isolation of stable phosphaalkenes [5,6]. Recently, such low-coordinated organophosphorus compounds should be one of the exciting research targets as new promising ligands toward transition metals in catalytic chemistry [3], since the low-coordinated phosphorus species exhibit low-lying π*-orbital level showing strong π-electron accepting character with effective trans-effect.

Recently, we have designed a novel β-ketophosphenato ligand, which is a heavier congener of β-ketiminato ligand, as a monovalent and bidentate ligand bearing an extremely bulky steric protection group, 2,4,6-tris[bis(trimethylsilyl)methyl]phenyl (denoted as Tbt) group, on the phosphorus atom (Scheme 2) [7]. It was demonstrated that the rhodium complex **2** coordinated with the β-ketophosphenato ligand was synthesized as a stable crystalline compound, showing strong trans-influence and trans-effect of the sp^2-hybridized phosphorus atom. Now, much attention has been focused on the heavier element analogue of β-diketiminato and imino-anilido ligands due to their expected features reflecting the

unique characters of both β-diketiminate-type skeleton and low-coordinated organophosphorus compounds (Scheme 1). While the complexation of an iminophospholido ligand with copper is known to give a unique cluster complex, the iminophospholido ligand did not work as a monovalent and bidentate ligand [8]. Although Mindiola et al. have postulated the existence of an intermediary titanium complex **3** bearing a P,N-chelating Schiff-base ligand (Scheme 3) [9], there has been no example for the isolation of a transition metal complex bearing such phosphorus analogue of a β-diketiminato ligand [10]. On the other hand, Ionkin et al. have reported the attempted synthesis of a phosphorus analogue of β-diketiminate **6** bearing 2,4,6-tri-*tert*-butylphenyl (denoted as Mes*) group [11]. However, it was suggested that **6** undergoes ready intramolecular cyclization to afford 1*H*-[1,2]diphosphole derivative **5** along with the elimination of Mes*H (Scheme 3). Taking this report into consideration, the more strained β-iminophosphido skeleton fused with a benzene ring may be helpful to avoid such intramolecular cyclization. Thus, we have designed benzo-fused P,N-chelating ligand **7** as a phosphorus analogue of a Schiff-base ligand (Scheme 4). In this case, however, the reaction of **9** with KH as a base afforded the corresponding 2-phospha-2*H*-isoindole **10** along with the elimination of Mes*H (Scheme 5) [12].

<insert Schemes 2-5 here>

In this paper, we report the synthesis of novel rhodium-carbonyl complexes **11** and **13**, which are isomeric complexes bearing different types of phosphorus analogues of Schiff-base ligands **7** and **8**, respectively, as stable crystalline compounds (Scheme 6). Their structures and properties were revealed on the basis of spectroscopic and X-ray crystallographic analyses, indicating the trans-influence of the low-coordinated phosphorus atoms.

<insert Scheme 6 here>

2. Results and Discussion

Two types of novel ligands **7** and **8** were designed as phosphorus analogues of Schiff-base type ligands, and we prepared **9** and **12** as their precursors. Since such secondary phosphine and phosphaalkene derivatives should have high liability to oxidation and self-oligomerization, bulky Mes* should be introduced on the phosphorus atom for the steric protection. Compound **9** was prepared according to the previously reported procedures [12]. Similarly, compound **12** was synthesized as shown in Scheme 7. The structures of **9** and **12** were reasonably supported by the spectroscopic and X-ray crystallographic analyses (Figures 1 and 2). Both **9** and **12** exhibit high planarity of the skeleton consisting of the central P, N, C atoms, the fused aromatic ring, and ipso-carbon atoms of Mes* and Dip groups. While the position of the hydrogen atom of the NH and PH moieties cannot be definitively determined due to the inherent principle of X-ray crystallographic analysis, the N=C moiety of **9** and the P=C moiety of **12** are oriented toward the PH and NH moieties, respectively, indicating the existence of weak N–H–P hydrogen bonding. The P–C1 and N=C3 bond lengths of **9** [1.8440(18) and 1.265(2) Å, respectively] are similar to those of typical P–C and N=C bond lengths and suggest little contribution of the resonance structure **9B** with effective π-conjugation shown in Scheme 8. Similarly, phosphaalkenylamine **12** dominantly exhibit the canonical structure of **12A** (Scheme 8) on the basis of its P=C3 and N–C1 bond lengths [1.687(2) and 1.372(3) Å, respectively], which are similar to those of (E)-Mes*P=CHPh [1.660(6) Å] [13] and typical diarylamines.

<insert Schemes 7 and 8 here>

<insert Figures 1 and 2 here>

In the ^{31}P NMR spectrum, compound **9** showed δ_P = –62.7 in the high field region similar to those of secondary phosphines. In the ^{1}H NMR spectrum of **9**, a characteristic doublet signal due to the P–H moiety was observed at 6.51 ppm with $^{1}J_{PH}$ = 258.3 Hz, which

is relatively low-field shifted as compared with those of diarylphosphines (around 5 ppm) [14], indicating the weak P–H–N hydrogen bonding. The signal due to the N=CH moiety was observed at δ_H = 8.53 as a doublet signal with $^4J_{PH}$ = 1.6 Hz. On the other hand, **12** showed a characteristically low-field shifted signal of δ_P = 241.2 in the ^{31}P NMR spectrum, supporting the sp^2-hybridized phosphorus atom with the P=C double bond character. In the ^{1}H NMR spectrum of **12**, the signal due to the P=CH moiety was observed at δ_H = 8.53 as a doublet signal with $^2J_{PH}$ = 23.7 Hz, which is similar to that of (E)-Mes*P=CHPh [the chemical shift of P=CH moiety is δ_H = 8.12 with $^2J_{PH}$ = 25.3 Hz] [15]. Interestingly, the N–H proton of **12** was observed at δ_H = 6.93, which is in lower field than that of diphenylamine (ca. 5.6 ppm) [16], as a doublet signal with the coupling constant of 20.7 Hz. The observed J coupling should be due to the through-space $^1J_{PH}$ coupling of the N–H–P moiety, strongly indicating the N–H–P hydrogen bonding. Thus, the structural and spectroscopic features of **9** and **12** suggested the little contribution of their canonical structures of B type (Scheme 8) and the N–H–P hydrogen bonding with the formation of the N–H–P–C–C–C ring system.

Attempted deprotonation reactions of **9** and **12** using *n*-BuLi and LDA were unsuccessful to give a complicated mixture, while **9** was found to be inert toward KH in THF at room temperature. However, heating of C_6D_6 suspension of **9** in the presence of KH at 60 ºC afforded 2-phospha-2*H*-isoindole **10** along with Mes*H as described above (Scheme 5) [12]. When **9** was treated with 0.5 eq. of $[RhCl(CO)_2]_2$ in THF at room temperature, the reaction proceeded slowly to give an unidentified complex X, which showed a characteristic signal at δ_P = –14.1 with $^1J_{PRh}$ = 164 Hz and $^1J_{PH}$ = 378 Hz in the ^{31}P NMR spectrum. Treatment of the reaction mixture with an excess amount of Et_3N at 60 ºC for 6 h afforded the rhodium-carbonyl complex **11** as a stable purple crystalline compound (Scheme 6). Similarly, heating of the C_6D_6 solution of **12** with 0.5 eq. of $[RhCl(CO)_2]_2$ in the presence of an excess amount of Et_3N afforded the corresponding rhodium-carbonyl complex **13** as a stable purple crystalline compound. Rhodium complexes **11** and **13** can be handled in the air without any decomposition probably due to the steric effect afforded by Mes* and Dip

(2,6-diisopropylphenyl) groups.

<insert Figures 3 and 4 here>

The structural parameters of rhodium-carbonyl complexes **11** and **13** were revealed by the X-ray crystallographic analysis (Figures 3-7). In the case of **11**, the P–C1 and C2–C3 bonds are shortened and the C1–C2 and C3–N bonds are elongated as compared with the corresponding bonds of **9**, suggesting the considerably delocalized π-electrons of the central six-membered ring skeleton of Rh–P–C–C–C–N. The sum of the internal angles of the Rh–P–C–C–C–N six-membered ring skeleton of **11** is 717º, showing its high planarity with the slightly pyramidalized phosphorus atom. The theoretically optimized structure of $\mathbf{11_{opt}}$ [17] is similar to that of **11** with the slightly pyramidalized phosphorus atom (the sum of the internal angles of the Rh–P–C–C–C–N six-membered ring skeleton of $\mathbf{11_{opt}}$ is 717º, Figure 7). However, the structural optimization of the less hindered model compound $\mathbf{11_{Me}}$ bearing a methyl group instead of Mes* group in **11** was found to have a highly distorted structure with a phosphorus atom showing a pyramidal geometry (the sum of the internal angles of the Rh–P–C–C–C–N six-membered ring skeleton is 686º). That is, the Mes* group of **11** should play an important role to afford the steric effect on the phosphorus atom for keeping the relatively planar geometry with sp^2-hybridization and preventing the phosphorus atom from pyramidalization. On the other hand, the structural parameters of the ligand moiety of **13** are similar to those of **12**, indicating the less electronic effect toward the ligand moiety by the complexation with a rhodium atom. That is, the N–C [1.374(6) Å] and P=C [1.666(5) Å] bond lengths of **13** are similar to those of **12** [N–C: 1.372(3) Å and P=C: 1.687(2) Å] in contrast to the case of **9** and **11** as described above. As in the case of **11**, the central six-membered ring skeleton of Rh–P–C–C–C–N of **13** exhibits an almost planar skeleton (the sum of the internal angles of the Rh–P–C–C–C–N six-membered ring skeleton is 720º), while the theoretically optimized structure of $\mathbf{13_{opt}}$ [17] is similar to those observed by the X-ray crystallographic analysis of **13**. However, the methyl-substituted model $\mathbf{13_{Me}}$ exhibits a

slightly twisted structure as in the case of **11$_{Me}$** (the sum of the internal angles of the Rh–P–C–C–C–N six-membered ring skeleton is 712º), suggesting the steric effect of Dip and Mes*. In both cases of **11** and **13**, the lengths of the Rh–CO bonds located at the trans-position of the phosphorus atom [1.943(4) Å for **11**, 1.933(5) for **13**] are longer than those located at the trans-position of the nitrogen atom [1.852(4) Å for **11** and 1.844(5) Å for **13**], suggesting the effective trans-influence of the coordinated phosphorus atom. Thus, it should be of great note that the two carbonyl groups on the rhodium center should be in non-equivalent situation in both cases of **11** and **13**, indicating the expectation of the novel reactivity of the rhodium-carbonyl complexes. In addition, the trans-influence of the phosphorus atom of **11** should be slightly stronger than that of **13** on the basis of their trans-C≡O bond lengths [1.106(4) Å for **11**, 1.131(5) Å for **13**].

<insert Figures 5-7 here>

The structural and electronic features of **11** and **13** in solution should be discussed on the basis of their NMR spectra. In ^{31}P NMR spectrum, **11** showed a surprisingly low-field shifted signal at δ_P = 91.9 with $^1J_{PRh}$ = 122 Hz, in contrast to those of rhodium-phosphine complexes (e.g., δ_P = 25.3 with $^1J_{PRh}$ = 127.3 Hz for [RhCl(PPh_3)($CO)_2$] (**14**)) [18], indicating the sp^2-character of the phosphorus atom of **11**. On the other hand, rhodium complex **13** showed a characteristic signal at δ_P = 158.6 with $^1J_{PRh}$ = 157 Hz, which is in the considerably low-field region as compared with that of **14** reflecting the P=C double bond character but in a region higher than that of precursor **12**.

The larger $^1J_{PRh}$ coupling constant of **13** ($^1J_{PRh}$ = 157 Hz) than that of [RhCl(PPh_3)($CO)_2$] (**14**, $^1J_{PRh}$ = 127.3 Hz) [18] should be due to the high s-character of the P-Rh bond of **13**, which may consist of the lone-pair of the phosphorus atom. Generally, the σ and π bonds of a phosphaalkene (RP=CR_2) exhibit high p-character and its lone pair dominantly consists of 3s orbital of the phosphorus atom, since a phosphorus atom has a tendency of keeping its intrinsic configuration of valence electrons, $(3s)^2(3p)^3$ [19].

Although the lone pair of PPh_3 should dominantly consist of 3s orbital of the phosphorus atom, the widened C–P–C angles than 90º due to the steric repulsion between the phenyl groups should enhance the p-character of the lone pair of PPh_3. Due to the less hindered situation of the phosphorus atom of a phosphaalkene as compared with PPh_3, the lone pair of a phosphaalkene exhibit higher s-character than that of PPh_3. Thus, the relatively large $^1J_{PRh}$ value of **13** should reflect the bonding properties of its P=C unit. On the other hand, the $^1J_{PRh}$ coupling constant of **11** ($^1J_{PRh}$ = 122 Hz) is similar to or slightly smaller than that of **14** ($^1J_{PRh}$ = 127.3), suggesting the higher p-character of the P–Rh bond of **11** than that of **14**. That is, the P–Rh bond should consist of sp^2-orbital of the phosphorus atom, suggesting that the lone pair of the phosphorus atom should exhibit high p-character and it should take part in the π-conjugation on the imino-phosphido ligand of **11**.

In ^{13}C NMR spectra, **11** showed two signals assignable to the carbonyl groups at δ_C = 185.7 ($^1J_{RhC}$ = 62.6 Hz, $^2J_{CP}$ = 97.3 Hz) and δ_C = 191.9 ($^1J_{RhC}$ = 67.1 Hz, $^2J_{CP}$ = 21.9 Hz). The former signal should be assignable to the CO group located at the trans-position of the phosphorus atom on the basis of the reported $^2J_{CP}$ values of $[RhCl(PPh_3)(CO)_2]$ (**14**, δ_C = 183.0, $^2J_{CP}$ = 16.3 for *cis*-CO for PPh_3, δ_C = 183.3, $^2J_{CP}$ = 123.4 Hz for *trans*-CO for PPh_3) [18]. The smaller $^1J_{RhC}$ value of the *trans*-CO for the phosphorus atom than that for the nitrogen atom should indicates the trans-influence of the phosphorus atom. Similarly, the ^{13}C NMR data for the CO groups of **13** were δ_C = 179.8 ($^1J_{RhC}$ = 65.4 Hz, $^2J_{CP}$ = 131.5 Hz, *trans*-CO for the phosphorus atom) and δ_C = 189.9 ($^1J_{RhC}$ = 58.1 Hz, $^2J_{CP}$ = 20.4 Hz, *cis*-CO for the phosphorus atom). The $^1J_{RhC}$ value of the *trans*-CO for the phosphorus atom is unexpectedly larger than that for the nitrogen atom, though the results of X-ray crystallographic analysis of **13** indicate the trans-influence of the phosphorus atom in the crystalline state. The reason for the relatively large $^1J_{RhC}$ value is not clear at present.

Preliminarily, we have performed the reaction of cyclohexanone with triethylsilane in the presence of a catalytic amount of **11** in the expectation that **11** can promote 1,4-hydrosilylation reaction even though **11** has CO groups on the rhodium atom. As a result, the treatment of cyclohexanone with 3 eq. of triethylsilane in the presence of 0.5 mol%

of **11** in benzene under reflux conditions for 4 h afforded the corresponding silylenolate **17** in an almost quantitative yield (Scheme 9) [20]. Thus, it was demonstrated that **11** can work as a catalyst for hydrosilylation probably due to the trans-effect of the phosphorus atom promoting the initial elimination of the trans-CO group for the phosphorus atom.

<insert Scheme 9 here>

3. Conclusion

We have designed novel P,N-chelating monovalent and bidentate ligands with an sp^2-hybridized phosphorus atom and succeeded in the synthesis of their rhodium-carbonyl complexes. The structural parameters of **11** and **13** suggested the effective trans-influence of their phosphorus atom. Interestingly, rhodium complexes **11** and **13**, which are isomers to each other and bear imino-phosphido and phosphaalkenyl-anilido ligands **7** and **8**, respectively, exhibited noticeable difference between their electronic properties on the basis of X-ray crystallographic and spectroscopic analyses. The preliminary demonstration using **11** toward catalytic hydrosilylation suggested that the imino-phosphido ligand **7** should be a possibly unique and attractive ligand for transition metals with strong trans-influence due to the sp^2-hybridized phosphorus atom. Further investigations on the synthesis of other transition metal complexes bearing such P,N-chelating ligands having an sp^2-phosphorus atom and the catalytic reactions using **11** and **13** are currently in progress.

4. Experimental

4.1. General procedure

All experiments were performed under an argon atmosphere unless otherwise noted. All solvents were purified by standard methods and then dried by using an Ultimate Solvent System (Glass Contour Company) [21]. All solvents used in the reactions and spectroscopy were dried by using a potassium mirror. ^{1}H NMR (300 MHz) and ^{13}C NMR (75 MHz) spectra were measured in $CDCl_3$ or C_6D_6 with a JEOL JNM AL-300 spectrometer. Signals

due to $CHCl_3$ (7.25 ppm) and C_6D_5H (7.15 ppm) were used as references in ^1H NMR, and those due to $CDCl_3$ (77 ppm) and C_6D_6 (128 ppm) were used in ^{13}C NMR. Multiplicity of signals in ^{13}C NMR spectra was determined by DEPT and CH-COSY techniques. ^{31}P NMR (120 MHz) spectra were measured in $CDCl_3$ or C_6D_6 with JEOL AL-300 spectrometer using 86% H_3PO_4 in water (0 ppm) as an external standard. All the P–H coupling constants were determined on the basis of both ^1H and non-decoupled ^{31}P NMR spectra. High resolution mass spectral data were obtained on a JEOL JMS-700 spectrometer (FAB) or a Bruker microTOF (ESI, APPI-TOF). Wet column chromatography (WCC) was performed with Wakogel C-200. All melting points were determined on a Yanaco micro melting point apparatus and were uncorrected. Elemental analyses were performed by the Microanalytical Laboratory of the Institute for Chemical Research, Kyoto University.

<insert Scheme 10 here>

4.1.1. Chlorophosphine **18** (Scheme 10)

To a THF solution (8 mL) of **14** (152 μL, 1.0 mmol) was added *n*-butyllithium (1.51 M hexane solution, 0.66 mL, 1.0 mmol) at –78 °C. After stirring at –78 °C for 30 min, a THF solution (8 mL) of Mes*PCl_2 (347 mg, 1.00 mmol) was added. The reaction mixture was gradually warmed up to room temperature and stirred for 3 h. After the removal of the solvent under the reduced pressure, the crude product was dissolved in hexane and then filtered through Celite®. The filtrate was purified with WCC (hexane/ether = 20/1) to afford **18** (271 mg, 0.588 mmol, 74%). **18**: pale yellow liquid; ^1H NMR (300 MHz, $CDCl_3$, 298 K) δ 1.33 (s, 9H), 1.35 (s, 18H), 3.58-3.66 (m, 2H), 3.87-3.93 (m, 2H), 4.05 (s, 1H), 7.29-7.35 (m, 2H), 7.39 (s, 2H), 7.47-7.52 (m, 1H), 7.83-7.87 (m, 1H); $^{13}C\{^1H\}$ NMR (75 MHz, $CDCl_3$, 298 K) δ 31.1 (CH_3), 33.8 (CH_3), 33.9 (CH_3), 34.8 (C), 39.9 (C), 84.8 (CH_2), 85.1 (CH_2), 100.0 (CH, d, $^3J_{PC}$ = 7.5 Hz), 124.0 (CH), 125.9 (CH), 128.7 (CH), 128.9 (CH), 131.9 (CH, d, J_{PC} = 8.3 Hz), 138.7 (CH, d, J_{PC} = 22.5 Hz), 139.0 (C), 139.8 (C), 152.8 (C), 161.1 (C, d, J_{PC} = 20.3 Hz); $^{31}P\{^1H\}$ NMR (120 MHz, $CDCl_3$, 298 K) δ 77.4. High-resolution MS (ESI): m/z

Calcd for $C_{27}H_{39}O_2PCl$ 461.2376. Found 461.2334 ($[M+H]^+$).

4.1.2. Diarylphosphine **19**

To a diethyl ether solution (10 mL) of **18** (123 mg, 0.267 mmol) was added lithium aluminum hydride (10 mg, 0.27 mmol) at 0 °C. The reaction mixture was gradually warmed up to room temperature and stirred for 30 min. Ethyl acetate was added to the reaction mixture for quench. After removal of the solvent under the reduced pressure, the crude product was dissolved in hexane and then filtered through Celite®. The purification of the filtrate with WCC (hexane/ether = 20/1) gave **19** (98 mg, 0.23 mmol, 85%). **19**: pale yellow liquid; ^{1}H NMR (300 MHz, $CDCl_3$, 298 K) δ 1.38 (s, 9H), 1.42 (s, 9H), 1.51 (s, 9H), 4.09-4.24 (m, 4H), 5.86 (dd, J = 4.0, 7.7 Hz, 1H), 6.12 (d, J_{PH} = 241.6 Hz, 1H), 6.28 (d, J = 4.2 Hz, 1H), 6.97 (dpt, J = 1.1, 7.7 Hz, 1H), 7.15 (pt, J = 7.5 Hz, 1H), 7.51-7.55 (m, 3H); ^{13}C{^{1}H} NMR (75 MHz, $CDCl_3$, 298 K) δ 31.5 (CH_3), 33.5 (CH_3), 35.3 (C), 38.6 (C), 65.4 (CH_2), 65.6 (CH_2), 102.4 (CH, J_{PC} = 20.3 Hz), 122.6 (CH), 125.4 (CH), 127.0 (CH), 127.6 (C), 128.0 (C), 128.8 (CH), 132.4 (CH), 138.2 (C, d, J_{PC} = 16.5 Hz), 139.8 (C, d, J_{PC} = 23.5 Hz), 150.8 (C); ^{31}P{^{1}H} NMR (120 MHz, $CDCl_3$, 298 K) δ –73.9. High-resolution MS (FAB): m/z Calcd for $C_{27}H_{39}O_2P$ 426.2688. Found. 426.2696 ($[M]^+$).

4.1.3. Ketophosphine **20**

An acetone solution (50 mL) of **19** (780 mg, 1.83 mmol) and *p*-toluenesulfonic acid monohydrate (32 mg, 0.18 mmol) was refluxed for 10 h. After the removal of the solvent under the reduced pressure, the purification of the crude product with WCC (hexane) gave **20** (523 mg, 1.37 mmol, 75%). **20**: yellow liquid; ^{1}H NMR (300 MHz, $CDCl_3$, 298 K) δ 1.37 (s, 9H), 1.45 (s, 18H), 5.97 (dd, J = 3.7, 7.3 Hz, 1H), 6.51 (d, $^1J_{PH}$ = 255.3 Hz, 1H), 7.18 (pt, J = 7.3 Hz, 1H), 7.29 (pt, J = 7.5 Hz, 1H), 7.53 (s, 1H), 7.54 (s, 1H), 7.78 (ddd, J = 1.4, 3.1, 7.5 Hz, 1H), 10.25 (d, $^4J_{PH}$ = 2.3 Hz, 1H); ^{13}C{^{1}H} NMR (75 MHz, $CDCl_3$, 298 K) δ 31.3 (CH_3), 33.3 (CH_3), 35.2 (C), 38.4 (C), 119.4 (C), 122.6 (CH), 126.6 (CH), 128.5 (C, d, J_{PC} = 29.0 Hz,), 132.8 (CH), 132.9 (CH), 134.0 (CH), 136.2 (C, d, J_{PC} = 9.3 Hz), 146.1 (C, d, J_{PC} = 34.6

Hz), 150.9 (C), 193.2 (CH, d, J_{PC} = 4.3 Hz); $^{31}P\{^{1}H\}$ NMR (120 MHz, $CDCl_3$, 298 K) δ –60.1. High-resolution MS (FAB): m/z Calcd for $C_{25}H_{35}OP$ 382.2426. Found. 382.2426 ($[M]^+$).

4.1.4. Compound **9**

To a toluene solution (5 mL) of **20** (50 mg, 0.13 mmol) was added $DipNH_2$ (250 μL, 1.3 mmol) and trifluoroborane diethyl etherate (14 μL, 0.11 mmol). After the reflux for 10 h, the solvent was removed under the reduced pressure. The purification of the crude product with WCC (hexane) gave **9** (69 mg, 0.12 mmol, 98%) [12].

4.1.5. Rhodium complex **11**

To a C_6H_6 solution (0.70 mL) of **9** (54 mg, 0.10 mmol) and $[RhCl(CO)_2]_2$ (19 mg, 0.049 mmol) was added triethylamine (140 μL, 1.0 mmol). The reaction mixture was heated at 60 °C for 6.0 h. The solvent was removed in vacuo. The purification of the crude product with Celite® filtration (hexane) gave **11** (69 mg, 0.12 mmol, 98%). **11**: deep purple crystals; m.p. 118 °C (decomp.); ^{1}H NMR (300 MHz, C_6D_6, 298 K) δ 0.98 (d, $^{3}J_{HH}$ = 7.2 Hz, 6H), 1.32 (d, $^{3}J_{HH}$ = 7.2 Hz, 6H), 1.33 (s, 9H), 1.77 (s, 18H), 3.36 (sept, $^{3}J_{HH}$ = 6.9 Hz, 6H), 6.61-6.67 (m, 1H), 6.72-6.79 (m, 1H), 7.07-7.28 (m, 5H), 7.85 (s, 1H), 7.86 (s, 1H), 8.10 (dd, J = 3.3, 5.1 Hz, 1H); $^{13}C\{1H\}$ NMR (75 MHz, C_6D_6, 298 K) δ 23.0 (CH_3), 25.1 (CH_3), 28.4 (CH), 31.4 (CH_3), 34.2 (CH_3), 35.3 (C), 40.2 (C), 120.1 (CH), 123.8 (CH), 124.3 (CH, d, J_{PC} = 8.0 Hz), 125.1 (C, d, J_{PC} = 16.1 Hz), 127.4 (C), 128.5 (CH), 129.0 (CH, d, J_{PC} = 9.3 Hz), 138.2 (CH, d, J_{PC} = 4.4 Hz), 139.7 (C), 150.7 (C, d, J_{PC} = 7.4 Hz), 151.8 (C, d, J_{PC} = 2.5 Hz), 157.1 (C, d, J_{PC} = 6.2 Hz), 161.1 (C), 161.6 (CH, d, J_{PC} = 16.1 Hz), 185.7 (C, dd, J = 62.6, 97.3 Hz), 191.9 (C, dd, J = 21.9, 67.1 Hz); $^{31}P\{^{1}H\}$ NMR (120 MHz, C_6D_6, 298 K) δ 91.9 (d, $^{1}J_{PRh}$ = 122 Hz); IR(KBr) ν_{CO} = 1988.7, 2045.78 cm^{-1}; High-resolution MS (FAB): m/z Calcd for $C_{39}H_{51}O_2NPRh$ 699.2712. Found 699.2724 ($[M]^+$); Anal. Calcd for $C_{39}H_{51}O_2NPRh$: C, 66.94; H, 7.35; N, 2.00%. Found: C, 66.85; H, 7.46; N, 2.05%.

4.1.6. Diarylamine **15**

To $DipNH_2$ (500 μL, 2.65 mmol) in toluene (6 mL) was added $Pd(OAc)_2$ (18 mg, 0.080 mmol), NaO(*t*-Bu) (443 mg, 4.62 mmol), DPEphos (64 mg, 0.12 mmol) and **1** (500 μL, 3.3 mmol). The reaction mixture was stirred at 120 °C for 8.0 h. The solvent was removed in vacuo. The purification of the crude product with Celite® filtration (hexane) and HPLC ($CHCl_3$) afforded **15** (648 mg, 1.99 mmol, 75%). **15**: pale yellow liquid; ^{1}H NMR (300 MHz, $CDCl_3$, 298 K) δ 1.16 (d, $^3J_{HH}$ = 6.9 Hz, 6H), 1.21 (d, $^3J_{HH}$ = 6.9 Hz, 6H), 3.19 (sept, $^3J_{HH}$ = 6.9 Hz, 2H), 4.10-4.21 (m,4H), 6.04 (s, 1H), 6.23 (d, J_{HH} = 8.4 Hz, 1H), 6.38 (s, 1H), 6.75 (t, $^3J_{HH}$ = 7.5 Hz, 1H), 7.10 (t, $^3J_{HH}$ = 6.6 Hz, 1H), 7.24-7.32 (m, 3H), 7.43 (d, $^3J_{HH}$ = 7.8 Hz, 1H); ^{13}C{^{1}H} NMR (75 MHz, $CDCl_3$, 298 K) δ 22.7 (CH_3), 24.5 (CH_3), 28.1 (CH), 64.7 (CH_2), 103.4 (CH), 112.4 (CH), 116.9 (CH), 120.6 (C), 123.6 (CH), 126.7 (CH), 127.0 (CH), 129.7 (C), 135.5 (C), 146.4 (C), 146.7 (C); High-resolution MS (EI): m/z Calcd for $C_{21}H_{27}O_2N$ 325.2042. Found. 325.2046 ($[M]^+$).

4.1.7. Diarylamine **16**

A toluene solution (10 mL) of **15** (197 mg, 0.605 mmol) and *p*-toluenesulfonic acid monohydrate (60 mg, 0.31 mmol) was stirred for 1.0 h. To the reaction mixture was added H_2O and extracted with toluene. The organic layer was dried with $MgSO_4$. The solvent was removed under the reduced pressure to afford **16** (165 mg, 0.586 mmol, 91%). **16**: yellow liquid; ^{1}H NMR (300 MHz, $CDCl_3$, 298 K) δ 1.11 (d, $^3J_{HH}$ = 6.9 Hz, 6H), 1.16 (d, $^3J_{HH}$ = 6.9 Hz, 6H), 3.07 (sept, $^3J_{HH}$ = 6.9 Hz, 2H), 6.23 (d, $^3J_{HH}$ = 8.7 Hz, 1H), 6.72 (t, $^3J_{HH}$ = 7.2 Hz, 1H), 7.20-7.36 (m, 3H), 7.56 (d, $^3J_{HH}$ = 7.8 Hz, 1H), 9.57 (s, 1H), 9.97 (s, 1H); ^{13}C{^{1}H} NMR (75 MHz, $CDCl_3$, 298 K) δ 23.0 (CH_3), 24.5 (CH_3), 28.4 (CH), 112.6 (CH), 115.7 (CH), 118.0 (C), 123.9 (CH), 128.0 (CH), 133.4 (C), 135.6 (CH), 136.2 (CH), 147.4 (C), 151.0 (C), 194.3 (C); High-resolution MS (EI): m/z Calcd for $C_{19}H_{23}ON$ 281.1780. Found. 281.1779 ($[M]^+$).

4.1.8. Compound **12** [22]

To a THF solution (10 mL) of Mes^*PH_2 (200 mg, 0.72 mmol) was added *n*-butyllithium (1.51

M hexane solution, 480 μL, 0.72 mmol) at –78 °C. After stirring at –78 °C for 15 min, the reaction temperature was raised up to room temperature and then the reaction mixture was stirred for 30 min. To the reaction mixture was added trimethylsilyl chloride (91 μL, 0.72 mmol) and keep stirring for 30 min. To the reaction mixture was added *n*-butyllithium (1.51 M hexane solution, 480 μL, 0.72 mmol). To the reaction mixture was added **16** at –78 °C and stirred for 3.0 h. After the removal of the solvent under the reduced pressure, the crude product was dissolved in hexane and then filtered through Celite®. The filtrate was purified with WCC (hexane) to afford **12** (85 mg, 0.16 mmol, 22%). **12**: yellow crystals, mp 192 °C (decomp.); ^{1}H NMR (300 MHz, $CDCl_3$, 298 K) δ 1.23 (d, $^{3}J_{HH}$ = 6.9 Hz, 6H), 1.30 (d, $^{3}J_{HH}$ = 6.9 Hz, 6H), 1.45 (s, 9H), 1.63 (s, 18H), 3.23 (sept, $^{3}J_{HH}$ = 6.9 Hz, 2H), 6.36 (d, $^{3}J_{HH}$ = 8.0 Hz, 1H), 6.73 (t, $^{3}J_{HH}$ = 7.4 Hz, 1H), 6.93 (d, J_{PH} = 20.7 Hz, 1H), 7.03 (t, $^{3}J_{HH}$ = 7.4 Hz, 1H), 7.17 (d, $^{3}J_{HH}$ = 8.0 Hz, 1H), 7.33-7.42 (m, 3H), 7.57 (s, 2H), 8.51 (d, $^{2}J_{PH}$ = 23.7 Hz, 1H); ^{13}C{^{1}H} NMR (75 MHz, $CDCl_3$, 298 K) δ 22.8 (CH_3), 25.1 (CH_3), 28.4 (CH), 31.4 (CH_3), 33.8 (CH_3), 33.9 (CH_3), 35.0 (C), 38.3 (C), 112.5 (CH), 116.8 (CH), 121.9 (CH), 123.9 (CH), 124.3 (C, d, J_{PC} = 3.1 Hz), 127.5 (CH), 128.6 (C, d, J_{PC} = 8.0 Hz), 132.0 (C, d, J_{PC} = 17.9 Hz), 135.0 (C), 139.9 (C, d, J_{PC} = 53.7 Hz), 146.5 (C), 147.4 (C), 149.9 (C), 154.1 (C), 176.6 (CH, d, J_{PC} = 38.9 Hz); ^{31}P{^{1}H} NMR (120 MHz, $CDCl_3$, 298 K) δ 241.2; High-resolution MS (EI): m/z Calcd for $C_{37}H_{52}NP$ 541.3837. Found. 541.3833 ($[M]^+$)**;** Anal. Calcd for $C_{37}H_{52}NP$: C, 82.02; H, 9.67; N, 2.59%. Found: C, 82.00; H, 9.74; N, 2.54%.

4.1.9. Rhodium Complex **13**

To a C_6H_6 solution (0.70 mL) of **12** (20 mg, 0.037 mmol) and $[RhCl(CO)_2]_2$ (7.3 mg, 0.019 mmol) was added triethylamine (50 μL, 0.37 mmol) at room temperature. The reaction mixture was heated at 60 °C for 4.0 h. The solvent was removed in vacuo. The purification of the crude product with Celite® filtration (hexane) gave **13** (29 mg, 0.036 mmol, 97%). **13**: purplish red crystals, mp 120 °C (decomp.); ^{1}H NMR (300 MHz, C_6D_6, 298 K) δ 1.03 (d, $^{3}J_{HH}$ = 7.2 Hz, 6H), 1.28 (s, 9H), 1.46 (d, $^{3}J_{HH}$ = 7.2 Hz, 6H), 1.73 (s, 18H), 3.29 (sept, $^{3}J_{HH}$ = 7.2 Hz, 6H), 6.47-6.51 (m, 1H), 6.77-6.80 (m, 1H), 6.85-6.91 (m, 1H), 7.02-7.05 (s,

1H), 7.22 (s, 3H), 7.74 (d, $^{3}J_{HH}$ = 3.3 Hz, 2H), 8.42 (d, $^{2}J_{PH}$ = 17.7 Hz, 1H); $^{13}C\{^{1}H\}$ NMR (75 MHz, C_6D_6, 298 K) δ 24.5 (CH_3), 24.8 (CH_3), 27.9 (CH), 30.9 (CH_3), 34.9 (CH_3), 35.4 (C), 39.4 (C), 115.1 (CH), 117.5 (CH), 1213.3 (CH, d, J_{PC} = 9.2 Hz), 124.0 (CH), 124.7 (CH), 126.3 (CH), 129.3 (C, d, J_{PC} = 27.8 Hz), 129.9 (CH), 134.1 (CH, d, J_{PC} = 24.1 Hz), 141.7 (C), 149.4 (C), 153.3 (C), 155.4 (CH, d, J_{PC} = 40.1 Hz), 156.7 (C), 163.0 (C); $^{31}P\{^{1}H\}$ NMR (120 MHz, C_6D_6, 298 K) δ 158.6 (d, $^{1}J_{PRh}$ = 157 Hz). High-resolution MS (ESI): m/z Calcd for $C_{38}H_{52}ONPRh$ 672.2836 ($[M+H]^+$). Found. 682.2841 ($[M-CO+H]^+$).

4.1.10. Hydrosilylation reaction

To a benzene solution (2 mL) of rhodium complex **11** (3.5 mg, 5.0 μmol) was added 2-cyclohexen-1-one (96 μL, 1.0 mmol) and Et_3SiH (480 μL, 3.0 mmol). The reaction mixture was heated at reflux temperature for 4 h. The solvent was removed in vacuo. The residue was purified with WCC (hexane) to afford silylenolate **17** (210 mg, 0.99 mmol, 99%) [23].

4.2. X-Ray crystallographic analysis

X-Ray crystallographic analysis of 9, 11, 12, and [13·C_6H_6]. The intensity data were collected on a Rigaku/MSC Mercury CCD diffractometer with graphite monochromated MoKα radiation (λ = 0.71070 Å). Single crystals suitable for X-ray analysis were obtained by slow recrystallization from hexane/THF (for **9** and **12**), benzene (for **11** and **[13·C_6H_6]**). The single crystals were mounted on a glass fiber. The structures were solved by a direct method (SIR-97 [24]) and refined by full-matrix least-squares procedures on F^2 for all reflections (SHELXL-97 [25]). All hydrogen atoms were placed using AFIX instructions, while all other atoms were refined anisotropically. Crystal data: **9**: $C_{37}H_{52}NP$, M = 541.77, T = 103(2) K, monoclinic, $P2_1/n$ (no.14), a = 9.8299(3) Å, b = 26.7647(6) Å, c = 13.2744(3) Å, β = 108.2538(12)°, V = 3316.67(15) $Å^3$, Z = 4, D_{calc} = 1.085 gcm^{-3}, μ = 0.107 mm^{-1}, $2\theta_{max}$ = 51.0, 29226 measured reflections, 6173 independent reflections (R_{int} = 0.0520), 420 refined parameters, GOF = 1.049, R_1 = 0.0447 and wR_2 = 0.1150 [$I>2\sigma(I)$], R_1 = 0.0710 and wR_2 =

0.1247 [for all data], largest diff. peak and hole 0.375 and -0.559 e.Å^{-3}. **11**: $C_{39}H_{51}NO_2PRh$, M = 699.69, T = 103(2) K, triclinic, P–1 (no.2), a = 9.149(3) Å, b = 10.890(4) Å, c = 20.211(7) Å, α = 97.934(4)º, β = 101.609(3)º, γ = 106.9868(16)º, V = 1844.4(10) Å^3, Z = 2, D_{calc} = 1.260 gcm^{-3}, μ = 0.538 mm^{-1}, $2\theta_{max}$ = 51.0, 16107 measured reflections, 6795 independent reflections (R_{int} = 0.0378), 410 refined parameters, GOF = 0.969, R_1 = 0.0387 and wR_2 = 0.1190 [I>2σ(I)], R_1 = 0. 0483 and wR_2 = 0.1337 [for all data], largest diff. peak and hole 0.602 and -0.771 e.Å^{-3}. **12**: $C_{37}H_{52}NP$, M = 541.77, T = 103(2) K, triclinic, P–1 (no.2), a = 9.484(3) Å, b = 13.720(4) Å, c = 13.737(4) Å, α = 93.542(2)º, β = 99.935(3)º, γ = 109.895(4)º, V = 1641.6(9) Å^3, Z = 2, D_{calc} = 1.096 gcm^{-3}, μ = 0.108 mm^{-1}, $2\theta_{max}$ = 51.0, 11551 measured reflections, 5989 independent reflections (R_{int} = 0.0329), 390 refined parameters, GOF = 1.069, R_1 = 0.0515 and wR_2 = 0.1094 [I>2σ(I)], R_1 = 0. 0746 and wR_2 = 0.1235 [for all data], largest diff. peak and hole 0.248 and -0.259 e.Å^{-3}. **[13·C_6H_6]**: $C_{45}H_{57}NO_2PRh$, M = 777.80, T = 113(2) K, orthorhombic, $P2_12_12_1$ (no.19), a = 9.5822(5) Å, b = 16.9794(11) Å, c = 24.7695(16) Å, V = 4030.0(4) Å^3, Z = 4, D_{calc} = 1.282 gcm^{-3}, μ = 0.500 mm^{-1}, $2\theta_{max}$ = 51.0, 35424 measured reflections, 7492 independent reflections (R_{int} = 0.0802), 452 refined parameters, GOF = 1.192, R_1 = 0.0498 and wR_2 = 0.0893 [I>2σ(I)], R_1 = 0. 0629 and wR_2 = 0.0963 [for all data], largest diff. peak and hole 0.742 and -0.559 e.Å^{-3}.

Appendix A. Supplementary data: CCDC 729128-729131 contains the supplementary crystallographic data for **9**, **11**, **12**, and **[13·C_6H_6]**, respectively. These data can be obtained free of charge via http://www.ccdc.cam.ac.uk/conts/retrieving.html, or from the Cambridge Crystallographic Data Centre, 12 Union Road, Cambridge CB2 1EZ, UK; fax: (+44) 1223-336-033; or e-mail: deposit@ccdc.cam.ac.uk.

5. Acknowledgment

This work was supported by Grant-in-Aid for Creative Scientific Research (No. 17GS0207), Science Research on Priority Areas (No. 20036024, "Synergy of Elements"), and the Global COE Program ("Integrated Materials Science", Kyoto University) from Ministry of Education, Culture, Sports, Science and Technology, Japan.

References

[1] For a review see: L. Bourget-Merle, M.F. Lappert, J.R. Severn, Chem. Rev. 102 (2002) 3031.

[2] For examples, see: (a) B.Y. Liu, C.Y. Tian, L. Zhang, W.D. Yan, W.J. Zhang, J. Polym. Sci. Pol. Chem. 44 (2006) 6243. (b) D. Zhang, G.X. Jin, L.H. Weng, F.S. Wang, Organometallics 23 (2004) 3270. (c) X.F. Li, K. Dai, W.P. Ye, L. Pan, Y.S. Li, Organometallics 23 (2004) 1223. (d) R. Andres, E. de Jesus, F.J. de la Mata, J.C. Flores, R. Gomez, J. Organomet. Chem. 690 (2005) 939. (e) J.K. Zhang, Z.F. Ke, F. Bao, J.M. Long, H.Y. Gao, F.M. Zhu, Q. Wu, J. Mol. Catal. A 249 (2006) 31.

[3] For examples, see: (a) P.L. Floch, Cood. Chem. Rev. 250 (2006) 627. (b) F. Ozawa, S. Kawagishi, T. Ishiyama, M. Yoshifuji, Organometallics 23 (2004) 1325. (c) F. Mathey, Angew. Chem. Int. Ed. 42 (2003) 1578. (d) M. Okazaki, A. Hayashi, C.F. Fu, S.T. Liu, F. Ozawa, Organometallics 28 (2009) 902. (e) J. Yorke, L. Wan, A.B. Xia, W.J. Zheng, Tetrahedron Lett. 48 (2007) 8843. (f) C. Müller, L.G. López, H. Kooijman, A.L. Spek, D. Vogt, Tetrahedron Lett. 47 (2006) 2017.

[4] For reviews, see: (a) L. Weber, Chem. Rev. 92 (1992) 1839. (b) P.P. Power, Chem. Rev. 99 (1999) 3463. (c) N. Tokitoh, J. Organomet. Chem. 611 (2000) 217. (d) P.P. Power, J. Organomet. Chem. 689 (2004) 3904. (e) T. Sasamori, N. Tokitoh, Dalton Trans. (2008) 1395.

[5] (a) K. Dimroth, P. Hoffmann, Angew. Chem. Int. Ed. 3 (1964) 384. (b) G. Becker, Z. Anorg. Allg. Chem. 423 (1976) 242. (c) T.C. Klebach, R. Lourens, F. Bickelhaupt, J. Am. Chem. Soc. 100 (1978) 4886.

[6] The first stable diphosphene has been synthesized and isolated by Yoshifuji et al., see: M. Yoshifuji, I. Shima, N. Inamoto, K. Hirotsu, T. Higuchi, J. Am. Chem. Soc. 103 (1981) 4587.

[7] T. Sasamori, T. Matsumoto, N. Takeda, N. Tokitoh, Organometallics 26 (2007) 3621.

[8] J. Grundy, B. Donnadieu, F. Mathey, J. Am. Chem. Soc. 128 (2006) 7716.

[9] F. Basuli, J. Tomaszewski, J.C. Huffman, D.J. Mindiola, J. Am. Chem. Soc. 125 (2003) 10170.

[10] (a) There have been a few reports on the theoretical calculations for a phosphorus analogue of a Schiff-base type ligand (phosphaalkenylphenoxide) from the viewpoint of catalytic activities, see: M.S.W. Chan, L.Q. Deng, T. Ziegler, Organometallics 19 (2000) 2741, T.Z. Zhang, D.W. Guo, S.Y. Jie, W.H. Sun, T. Li, X.Z. Yang, J. Polym. Sci. Pol. Chem. 42 (2004) 4765. (b) Recently, anilido-phosphiniimine complexes have been synthesized, see: K.D. Conroy, W.E. Piers, M. Parvez, J. Organomet. Chem. 693 (2008) 834.

[11] A.S. Ionkin, W.J. Marshall, B.M. Fish, M.F. Schiffhauer, F. Davidson, C.N. McEwen, D.E. Keys, Organometallics 26 (2007) 5050.

[12] N. Tokitoh, T. Matsumoto, T. Sasamori, Heterocycles 76 (2008) 981.

[13] M. Yoshifuji, K. Toyota, I. Matsuda, T. Niitsu, N. Inamoto, K. Hirotsu, T. Higuchi, Tetrahedron 44 (1988) 1363.

[14] For examples, see: (a) Y. Yokoyama, K. Takahashi, Bull. Chem. Soc. Jpn. 60 (1987) 3485. (b) E. Rivard, A.D. Sutton, J.C. Fettinger, P.P. Power, Inorg. Chim. Acta 360 (2007) 1278.

[15] M. Yoshifuji, K. Toyota, N. Inamoto, Tetrahedron Lett. 26 (1985) 1727.

[16] SDBSWeb: http://riodb01.ibase.aist.go.jp/sdbs/ (National Institute of Advanced Industrial Science and Technology, April, 2009)

[17] All calculations were conducted using the Gaussian 03 series of electronic structure programs. The geometries were optimized with density functional theory at the B3PW91 level using 6-31G(d) basis sets (for C, H, N, and O), 6-311G(3d) (for P), and Lanl2DZ (for Rh). It was confirmed by frequency calculations that the optimized structures have minimum energies. Computation time was provided by the Super Computer Laboratory, Institute for Chemical Research, Kyoto University.

[18] E. Rotondo, G. Battaglia, G. Giordano, F.P. Cusmano, J. Organomet. Chem. 450 (1993) 245.

[19] T. Sasamori, E. Mieda, N. Nagahora, K. Sato, D. Shiomi, T. Takui, Y. Hosoi, Y. Furukawa, N. Takagi, S. Nagase, N. Tokitoh, J. Am. Chem. Soc. 128 (2006) 12582, and references cited therein.

[20] Some control experiments have been examined as follows: (i) Reaction of 2-cyclohexen-1-one (96 μL, 1.0 mmol) with Et_3SiH (480 μL, 3.0 mmol) in benzene (2 mL) in the absence of any catalysis under the reflux conditions for 4 h. (ii) Reaction of 2-cyclohexen-1-one (96 μL, 1.0 mmol) with Et_3SiH (480 μL, 3.0 mmol) in benzene (2 mL) in the presence of ligand **9** (2.7 mg, 5.0 μmol) under the reflux conditions for 4 h. (iii) Reaction of 2-cyclohexen-1-one (96 μL, 1.0 mmol) with Et_3SiH (480 μL, 3.0 mmol) in benzene (2 mL) in the presence of $[RhCl(CO)_2]_2$ (1.0 mg, 2.5 μmol) under the reflux conditions for 4 h. All of these control reactions were unsuccessful with the quantitative recover of 2-cyclohexen-1-one.

[21] A. B. Pangborn, M. A. Giardello, R. H. Grubbs, R. K. Rosen, F. J. Timmers, Organometallics 15 (1996) 1518.

[22] For the recent development on phospha-Peterson reactions, see: M. Yam, J.H. Chong, C.W. Tsang, B.O. Patrick, A.E. Lam, D.P. Gates, Inorg. Chem. 45 (2006) 5225, and references cited therein.

[23] I. Ojima, R. J. Donovan, N. Clos, Organometallics 10 (1991) 2606.

[24] A. Altomare, M.C. Burla, M. Camalli, G.L. Cascarano, C. Giacovazzo, A. Guagliardi, A.G.G. Moliterni, G. Polidori, R. Spagna, Journal of Applied Crystallography 32 (1999) 115.

[25] (a) G.M. Sheldrick, Acta Crystallographica Section A 46 (1990) 467. (b) G. Sheldrick, SHELX-97 Program for Crystal Structure Solution and the Refinement of Crystal Structures, Institüt für Anorganische Chemie der Universität Göttingen, Tammanstrasse 4, D-3400 Göttingen, Germany, 1997.

< Figures and Schemes >

Scheme 1

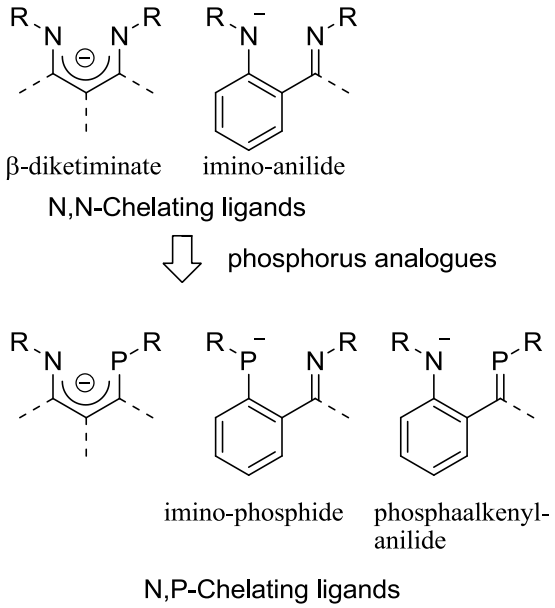

Scheme 2

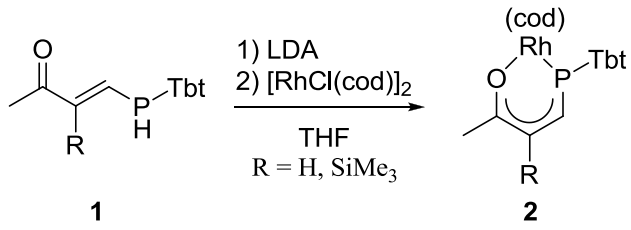

1 **2**

Tbt = 2,4,6-tris[bis(trimethylsilyl)methyl]phenyl
cod = cyclooctadiene

Scheme 3

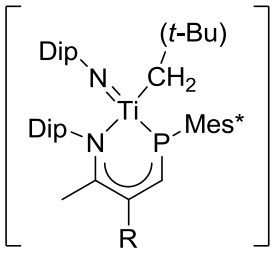

3

proposed as a possible intermediate

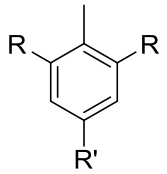

Mes*: R = R' = *t*-Bu
Dip: R = *i*-Pr, R' = H

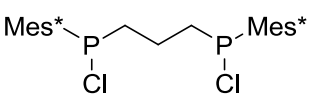

4

base
– HCl
– Mes*H

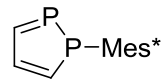

5

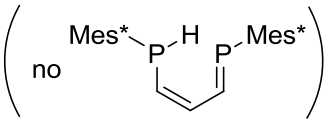

6

Scheme 4

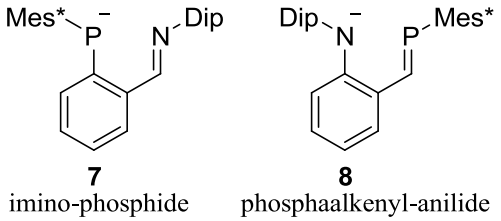

7 imino-phosphide **8** phosphaalkenyl-anilide

Schiff-base type N,P-chelating ligands

Scheme 5

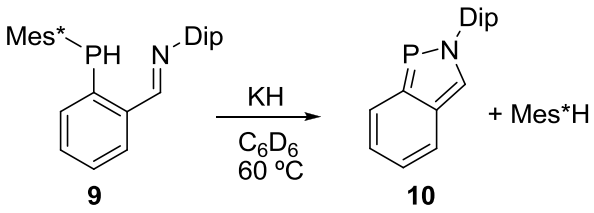

9 **10**

Scheme 6

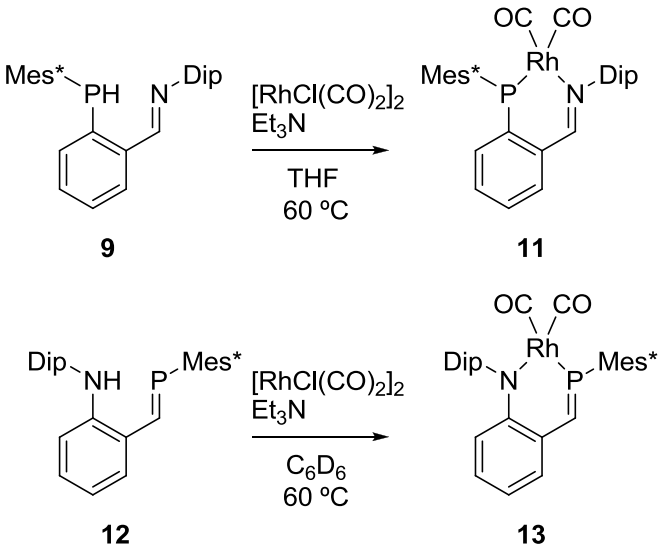
Mes*
PH
N
Dip
[RhCl(CO)2]2
Et3N
THF
60 ºC
OC
CO
Rh
Mes*
P
N
Dip
9
11
Dip
NH
P
Mes*
[RhCl(CO)2]2
Et3N
C6D6
60 ºC
OC
CO
Rh
Dip
N
P
Mes*
12
13

Scheme 7

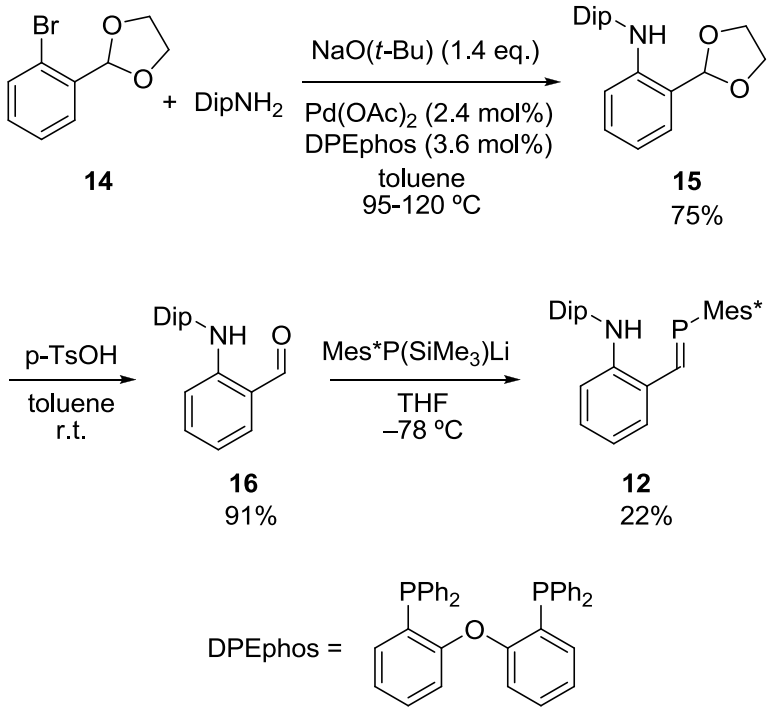
Br
O
O
+ DipNH2
NaO(t-Bu) (1.4 eq.)
Pd(OAc)2 (2.4 mol%)
DPEphos (3.6 mol%)
toluene
95-120 ºC
Dip
NH
O
O
14
15
75%
p-TsOH
toluene
r.t.
Dip
NH
O
16
91%
Mes*P(SiMe3)Li
THF
–78 ºC
Dip
NH
P
Mes*
12
22%
DPEphos =
PPh2
PPh2
O

Scheme 8

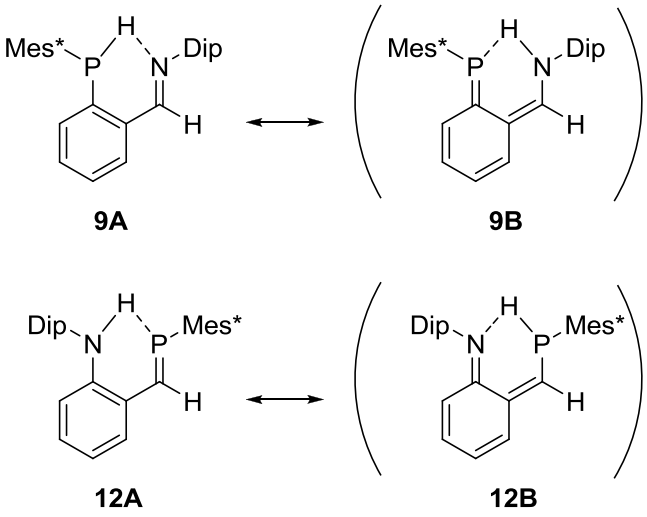
Mes*
H
P
N
Dip
H
Mes*
H
P
N
Dip
H
9A
9B
Dip
H
N
P
Mes*
H
Dip
H
N
P
Mes*
H
12A
12B

Scheme 9.

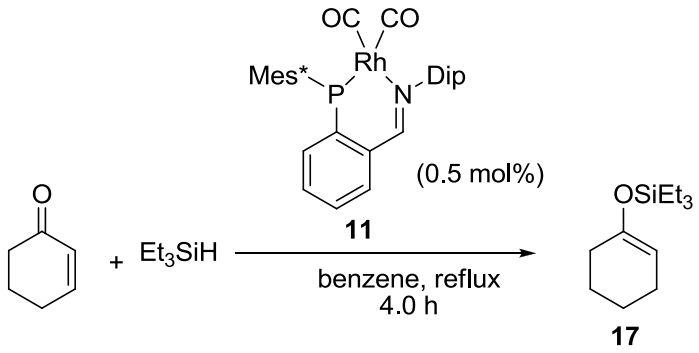
OC
CO
Rh
Mes*
P
N
Dip
(0.5 mol%)
11
O
+ Et3SiH
benzene, reflux
4.0 h
OSiEt3
17

Scheme 10.

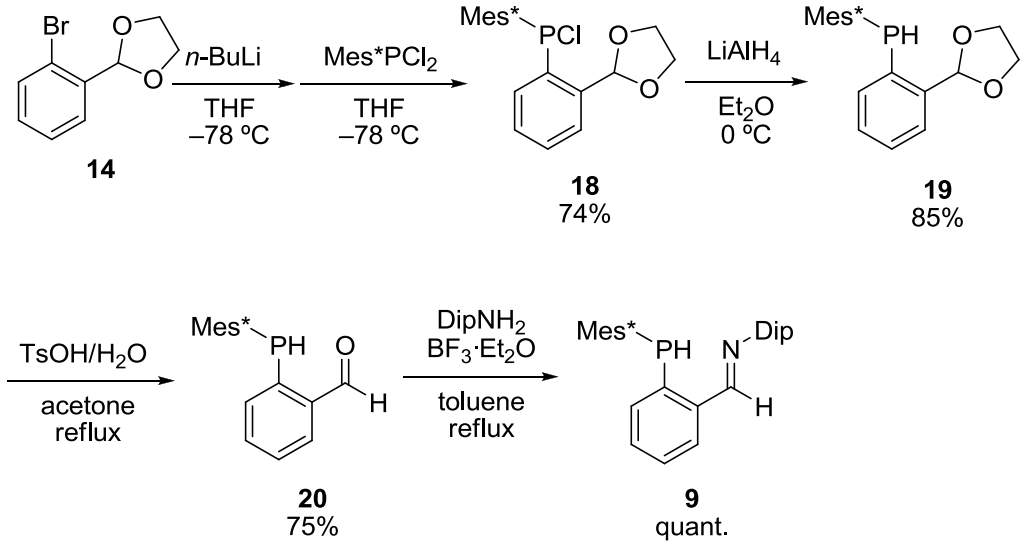
Br
O
O
14
n-BuLi
THF
–78 °C
Mes*PCl2
THF
–78 °C
Mes*
PCl
O
O
18
74%
LiAlH4
Et2O
0 °C
Mes*
PH
O
O
19
85%
TsOH/H2O
acetone
reflux
Mes*
PH
O
H
20
75%
DipNH2
BF3·Et2O
toluene
reflux
Mes*
PH
N
Dip
H
9
quant.

Figure 1. Molecular structure of **9**. Displacement ellipsoids were drawn at the 50% level. Hydrogen atoms were omitted for clarity. Selected bond lengths (Å) and angles (deg): P–C1, 1.8440(18); P–C(Mes*), 1.8475(7); N–C3, 1.265(2), N–C(Dip), 1.428(2); C1–C2, 1.417(2); C2–C3, 1.465(2); (Mes*)C–P–C1, 100.33(7); P–C1–C2, 121.37(12); C1–C2–C3, 123.37(15); C2–C3–N, 123.45(15); C3–N–C(Dip), 119.36(14).

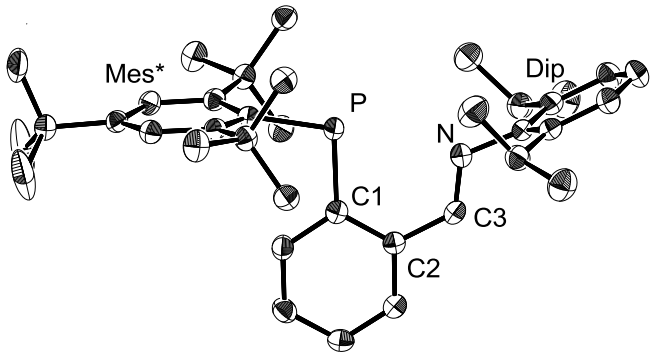

Figure 2. Molecular structure of **12**. Displacement ellipsoids were drawn at the 50% level. Hydrogen atoms were omitted for clarity. Selected bond lengths (Å) and angles (deg): N–C1, 1.372(3); N–C(Dip), 1.432(3); P–C3, 1.687(2), P–C(Mes*), 1.841(2); C1–C2, 1.425(3); C2–C3, 1.454(3); (Dip)C–N–C1, 124.49(17); N–C1–C2, 120.58(18); C1–C2–C3, 124.47(18); C2–C3–P, 129.24(16); C3–P–C(Mes*), 102.62(9).

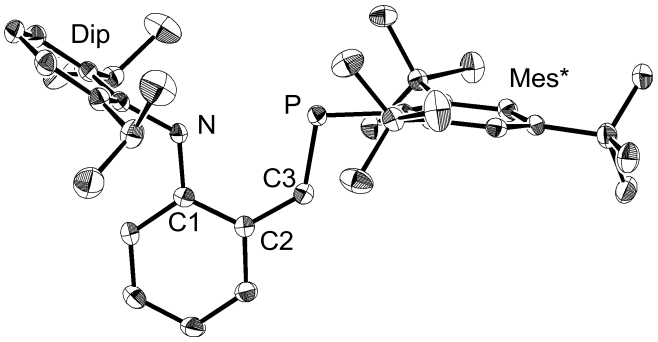

Figure 3. Molecular structure of **11**. Displacement ellipsoids were drawn at the 50% level. Hydrogen atoms were omitted for clarity. Selected bond lengths (Å) and angles (deg): P–Rh, 2.2665(11); N–Rh, 2.080(3); Rh–C4, 1.852(4); Rh–C5, 1.943(4); C4–O1, 1.142(4); C5–O2, 1.106(4); P–C1, 1.768(3); P–C(Mes*), 1.840(3); N–C3, 1.308(4), N–C(Dip), 1.452(4); C1–C2, 1.424(4); C2–C3, 1.432(4); P–Rh–N, 89.93(7); Rh–P–C1, 116.64(10); Rh–N–C3, 132.5(2); (Mes*)C–P–C1, 109.62(15); P–C1–C2, 121.6(2); C1–C2–C3, 126.2(3); C2–C3–N, 130.0(3); C3–N–C(Dip), 114.0(3).

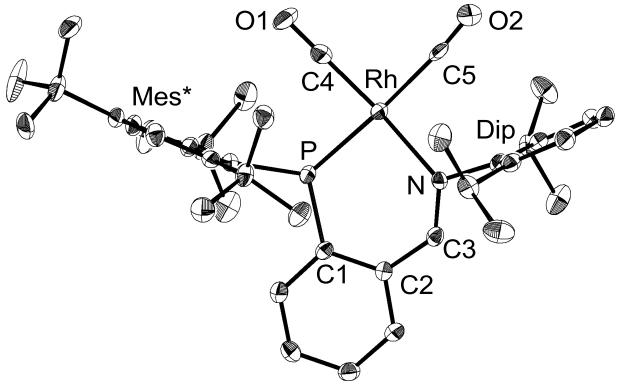

Figure 4. Molecular structure of **13**. Displacement ellipsoids were drawn at the 50% level. Hydrogen atoms were omitted for clarity. Selected bond lengths (Å) and angles (deg): P–Rh, 2.2261(12); N–Rh, 2.066(4); Rh–C4, 1.933(5); Rh–C5, 1.844(5); C4–O1, 1.131(5); C5–O2, 1.143(6); N–C1, 1.374(6); N–C(Dip), 1.450(6); P–C3, 1.666(5), P–C(Mes*), 1.818(5); C1–C2, 1.435(7); C2–C3, 1.428(7); N–Rh–P, 88.29(11); Rh–N–C1, 136.6(3); Rh–P–C3, 118.91(17); (Dip)C–N–C1, 115.3(4); N–C1–C2, 124.0(4); C1–C2–C3, 125.5(4); C2–C3–P, 126.6(4); C3–P–C(Mes*), 110.5(2).

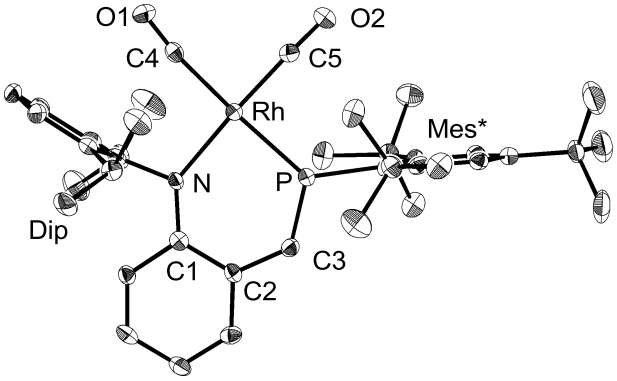

Figure 5. (a) Observed structure of **11**. (b) Optimized structure of $\mathbf{11_{opt}}$ [17]. (c) Optimized structure of $\mathbf{11_{Me}}$ [17].

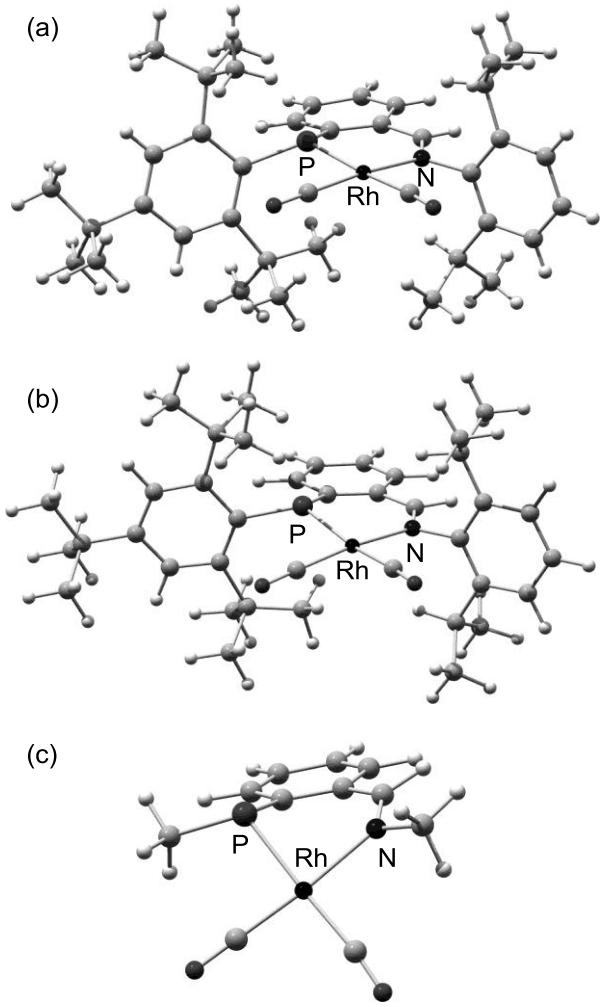

Figure 6. (a) Observed structure of **13**. (b) Optimized structure of $\mathbf{13}_{\mathbf{opt}}$ [17]. (c) Optimized structure of $\mathbf{13}_{\mathbf{Me}}$ [17].

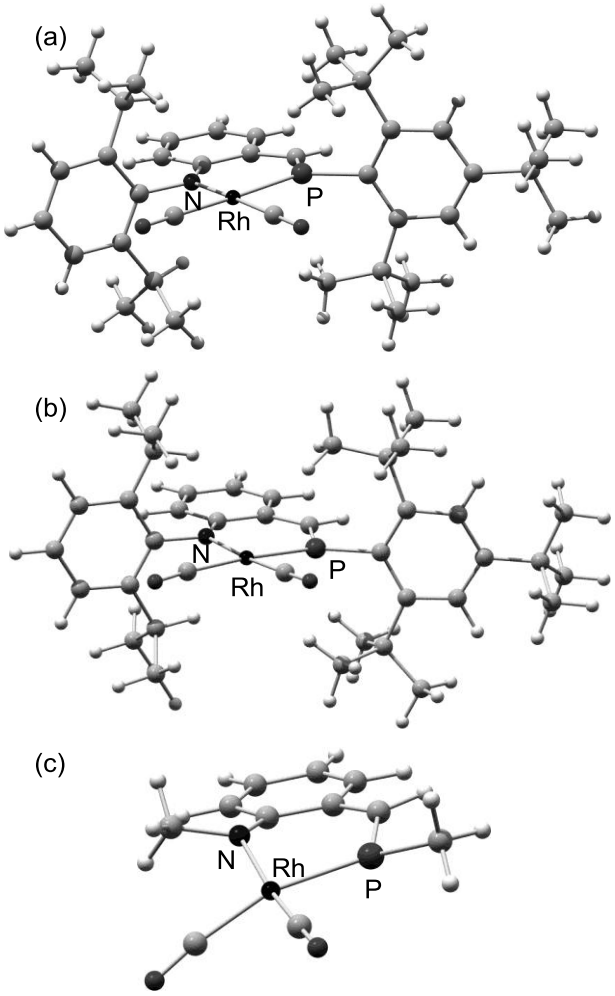

Figure 7. Summary of observed and optimized structural parameters of **11**, **11_{opt}**, **11_{Me}**, **13**, **13_{opt}**, and **13_{Me}** [17]. *The sum of internal angles of the Rh–P–C–C–C–N six-membered ring skeleton.

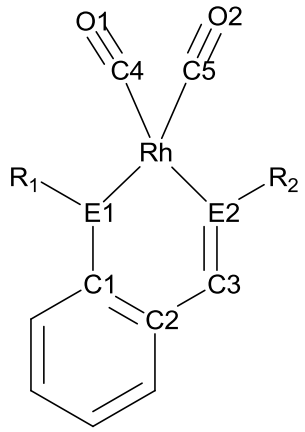

	11	**11_{opt}**	**11_{Me}**	**13**	**13_{opt}**	**13_{Me}**
Rh–E1/Å	2.2665(11)	2.300	2.349	2.066(4)	2.111	2.088
Rh–E2/Å	2.080(3)	2.122	2.163	2.2261(12)	2.269	2.271
E1–C1/Å	1.768(3)	1.767	1.818	1.374(6)	1.367	1.359
C1–C2/Å	1.424(4)	1.431	1.424	1.435(7)	1.448	1.451
C2–C3/Å	1.432(4)	1.432	1.450	1.428(7)	1.421	1.416
C3–E2/Å	1.308(4)	1.308	1.289	1.666(5)	1.675	1.685
Rh–C4/Å	1.852(4)	1.861	1.848	1.933(5)	1.943	1.926
Rh–C5/Å	1.943(4)	1.931	1.932	1.844(5)	1.860	1.871
C4–O1/Å	1.142(4)	1.152	1.153	1.131(5)	1.146	1.149
C5–O2/Å	1.106(4)	1.150	1.151	1.143(6)	1.153	1.153
Σ*	717°	717°	686°	720°	720°	712°

Graphical abstract

Schiff-base type N,P-chelating ligands, i.e., phosphorus analogues of imino-anilido ligands, were designed and synthesized as a new type of ligands toward a transition metal. Complexation reactions of the novel imino-phosphido and phosphaalkenyl-anilido ligands with $[RhCl(CO)_2]_2$ resulted in the formation of the corresponding rhodium-carbonyl complexes as stable crystalline compounds, the unique structural and electronic features of which were revealed based on their spectroscopic and X-ray crystallographic analyses.